LETTERS

Patterning organic single-crystal transistor arrays

Alejandro L. Briseno[1,2], Stefan C. B. Mannsfeld[1], Mang M. Ling[1], Shuhong Liu[1], Ricky J. Tseng[2], Colin Reese[1], Mark E. Roberts[1], Yang Yang[2], Fred Wudl[2] & Zhenan Bao[1]

Field-effect transistors made of organic single crystals are ideal for studying the charge transport characteristics of organic semiconductor materials[1]. Their outstanding device performance[2–8], relative to that of transistors made of organic thin films, makes them also attractive candidates for electronic applications such as active matrix displays and sensor arrays. These applications require minimal cross-talk between neighbouring devices. In the case of thin film systems, simple patterning of the active semiconductor layer[9,10] minimizes cross-talk. But when using organic single crystals, the only approach currently available for creating arrays of separate devices is manual selection and placing of individual crystals—a process prohibitive for producing devices at high density and with reasonable throughput. In contrast, inorganic crystals have been grown in extended arrays[11–13], and efficient and large-area fabrication of silicon crystalline islands with high mobilities for electronic applications has been reported[14,15]. Here we describe a method for effectively fabricating large arrays of single crystals of a wide range of organic semiconductor materials directly onto transistor source–drain electrodes. We find that film domains of octadecyltriethoxysilane microcontact-printed onto either clean Si/SiO_2 surfaces or flexible plastic provide control over the nucleation of vapour-grown organic single crystals. This allows us to fabricate large arrays of high-performance organic single-crystal field-effect transistors with mobilities as high as $2.4\,cm^2\,V^{-1}\,s^{-1}$ and on/off ratios greater than 10^7, and devices on flexible substrates that retain their performance after significant bending. These results suggest that our fabrication approach constitutes a promising step that might ultimately allow us to utilize high-performance organic single-crystal field-effect transistors for large-area electronics applications.

Figure 1a illustrates the single-crystal patterning process (see Methods for a detailed description). First, thick octadecyltriethoxysilane (OTS) films (average thickness $\sim 13 \pm 2$ nm, measured by ellipsometry) are printed by microcontact printing onto a clean SiO_2/Si substrate, using a polydimethylsiloxane (PDMS) stamp with a relief structure in the desired pattern. We note that although the results discussed here mainly relate to structures grown on arrays of micrometre-sized OTS squares, it is straightforward to create more-complex OTS film patterns for single-crystal nucleation (Supplementary Figs 3 and 6). After film deposition, crystals are grown using a vapour transport method[16] applicable to a broad range of materials, including high-mobility p-type materials such as rubrene, pentacene and tetracene, and n-type materials such as C_{60}, fluorinated copper phthalocyanine ($F_{16}CuPc$) and tetracyanoquinodimethane (TCNQ) (Supplementary Fig. 14). We find that sublimation of the organic material and crystal growth are accomplished in as little as five minutes for pentacene and as much as two hours for C_{60}, and that crystal nucleation is restricted to OTS-stamped regions and not observed on the SiO_2 background. The crystals show strong birefringence in optical micrographs recorded under cross-polarized light (Supplementary Fig. 6), confirming their crystalline nature. We also observe intense and narrow diffraction peaks in the X-ray diffraction patterns of pentacene, rubrene and C_{60} single crystals, which are indicative of a high degree of crystallinity (Supplementary Figs 5, 8 and 12).

Examples of arrays of single crystals of pentacene, rubrene and C_{60} grown on stamped OTS domains are shown in Fig. 1b–d. The growth of discrete single crystals is achieved by controlling the feature size of the printed OTS regions so that it supports on average only one crystal nucleation event. In the case of pentacene, crystal nucleation activity as a function of the size of the stamped OTS domains was analysed by using arrays of OTS squares with areas of $25\,\mu m^2$ (that is, $5 \times 5\,\mu m$), $625\,\mu m^2$ ($25 \times 25\,\mu m$), $2{,}500\,\mu m^2$ ($50 \times 50\,\mu m$) and $10{,}000\,\mu m^2$ ($100 \times 100\,\mu m$). To ensure that crystallization can be accurately compared on different active areas, a special PDMS stamp was fabricated containing four different feature sizes on one stamp, thus preventing sample-to-sample variations. The results are summarized in Fig. 2a, which plots the average number of nuclei (as counted in numerous fields of each stamp size) versus the stamped domain area. Within experimental error, the data fit a line corresponding to a constant nucleation density of about one nucleus per $49\,\mu m^2$, or a single pentacene crystal per $7 \times 7\,\mu m$ domain area. This finding is in good agreement with our finding that the $5 \times 5\,\mu m$ stamp (used to generate the array shown in Fig. 1b) yields approximately one single crystal per domain. The images in Fig. 2b show the results of using a large-area array of $5 \times 5\,\mu m$ stamped OTS domains for controlling pentacene growth, demonstrating that most patterns result in the formation of discrete pentacene single crystals.

OTS surface treatments have previously been used to pattern pentacene thin films on structured substrates. In the case of preferential pentacene thin film growth on OTS-treated gold surface structures[17], selective film growth was attributed to different surface interactions and surface diffusivities. Patterning SiO_2 substrates with OTS and FDTS ((heptadecafluorotetrahydrodecyl)trichlorosilane) also results in patterned growth of pentacene films[9]: within a certain window of growth conditions, pentacene forms two-dimensional islands (islands with monolayer-stepped terraces) on the patterned OTS regions, but only three-dimensional islands (disconnected single grains) in the FDTS-treated regions. These locally different modes of pentacene film growth were attributed to different molecule–substrate interactions.

However, the present study investigates the patterning of discrete single crystals, rather than the formation and patterning of thin films[18,19], and the selectivity achieved in our systems is more likely to be due to the high roughness of the thick OTS-stamped film rather than to different molecule–substrate interactions arising from a contrast in surface chemistry. This view is supported by atomic force microscope images typically showing an r.m.s. roughness of ~ 150 Å in the stamped OTS domains (Supplementary Fig. 1), and an r.m.s. roughness of < 5 Å in regions of bare SiO_2. In control experiments

[1]Department of Chemical Engineering, Stanford University, Stanford, California 94305, USA. [2]Department of Chemistry and Biochemistry and Exotic Materials Institute, Department of Materials Science and Engineering, University of California-Los Angeles, Los Angeles, California 90095, USA.

using thick OTS films stamped onto a vapour-deposited smooth OTS monolayer background (r.m.s. roughness <2 Å), pentacene crystals nucleated only in the patterned regions and with the same selectivity as seen with thick OTS film patterns stamped on bare SiO_2 (Supplementary Fig. 15). These observations agree with classical nucleation theory, which predicts that the higher surface energy associated with irregularities such as indentions, step edges or protrusions significantly lowers the barrier to heterogeneous nucleation, relative to that on a flat surface[20,21]; they also agree with a modern phase field theory, which similarly predicts heterogeneous nucleation to favourably occur on rough surfaces[22,23]. However, we note that besides the rough topology of the OTS-stamped domains, the use of a rather high substrate temperature is also important in achieving selective crystal growth. The substrate temperature, which is only ~20 °C lower than that of the evaporation source, results in a higher thermal redesorption rate in the bare SiO_2 regions than in the adjacent rough OTS regions. Given the large number of molecules required to form a stable nucleus at high substrate temperatures[9,24], nucleation on the bare SiO_2 surface is effectively suppressed. Consequently, the nucleation of crystals is effectively suppressed in smooth regions, while the stamped rough OTS domains act as effective primary nucleation centres. This interpretation is supported by inspection of the underside of the crystal making direct contact with the OTS film, which revealed that the initial nucleus may have grown from the valley of the rough OTS film in a conformal fashion, with large parts of the bottom surface being planar and in close contact to the substrate (Supplementary Figs 17, 18).

The control over crystal nucleation and growth provided by the OTS patterns makes it possible to grow large arrays of crystals directly onto transistor source–drain electrodes (see also Methods). This is illustrated in Fig. 3a, which shows rubrene single crystals patterned into a 14 × 14 transistor array. In most cases a few crystals are found between each pair of source and drain electrodes, but in some cases just one rubrene single crystal bridges the channel region (optical micrograph in Fig. 3b). One-step fabrication of large arrays of transistors with a single crystal in the channel region has until now been impossible to achieve with any of the reported methods of single-crystal field-effect transistor fabrication[1]. More than 99% of the devices with at least one crystal bridging the drain and source electrodes exhibited a field effect, with the electrical characteristics of the highest-mobility rubrene device shown in Fig. 3b. Overall, measured mobility values range from 0.1 to 2.4 $cm^2 V^{-1} s^{-1}$. This large variability may be partly attributed to the marked anisotropy of charge transport in rubrene[7] and to differences in contact quality at the dielectric/semiconductor and electrode/semiconductor interfaces.

The crystals are able to make contact because the stamped OTS on both Au and SiO_2 consists of sparse pillars that do not fully coat the surface. Moreover, some of the OTS stamped on Au was found to evaporate on heating under conditions similar to those used during crystal growth (Supplementary Fig. 19). The growing crystal itself also seems to push some OTS pillars outside the stamping field, thereby leaving a visible outline of the peeled-off crystal on the substrate (Supplementary Fig. 20); this effect increases the contact area between the crystal and the dielectric and electrode surfaces. But the calculated mobilities may nevertheless underestimate the true mobilities, because it is still possible that only portions of the bottom surface of the crystal make contact with the dielectric surface. Nonetheless, random testing of 22 of the devices in the 14 × 14

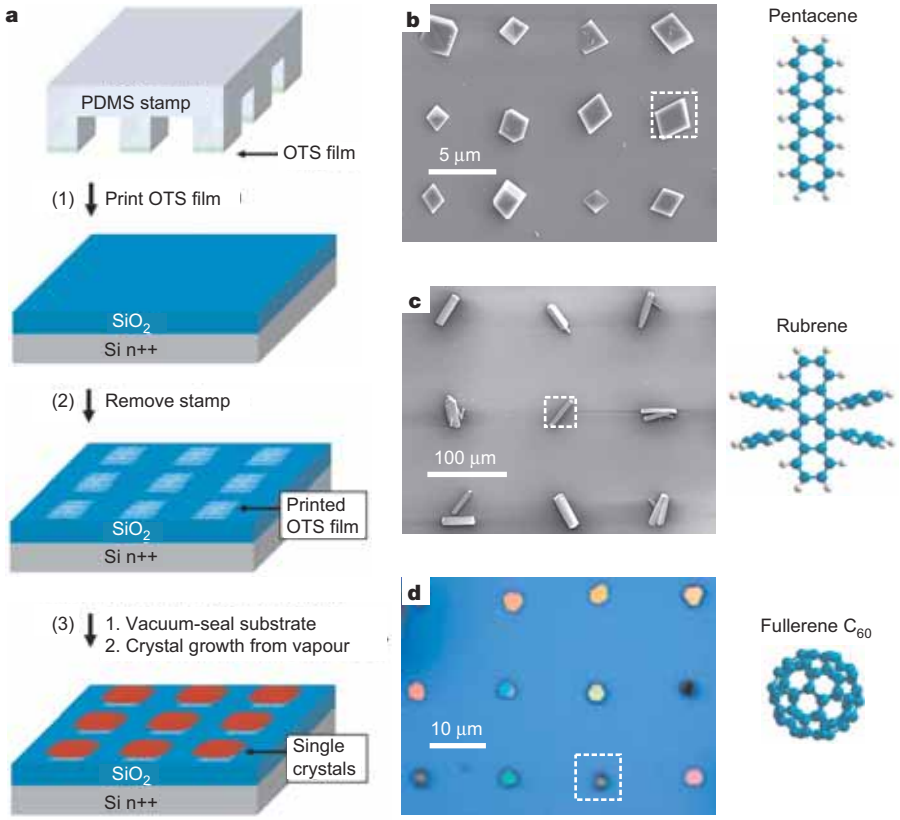

Figure 1 | Patterning of organic single crystals. **a**, Schematic outline of the procedure used to grow organic single crystals on substrates that have been patterned by microcontact printing. The printing uses PDMS stamps with relief features that are inked with a thick OTS film and then pressed onto the substrates. To grow the patterned single crystals, the patterned substrate is placed in a glass tube with the organic source material, vacuum-sealed (0.38 mm Hg), and placed in a temperature gradient furnace tube. **b**–**d**, Patterned single-crystal arrays of different organic semiconductor materials. The dotted square in each image indicates the size and location of one of the OTS-stamped domains, while the molecular structure of the organic material used is shown next to the image of its single-crystal array. **b**, Pentacene (scanning electron microscope, SEM, image; stamped domain size 4 × 4 μm); **c**, rubrene (SEM, 25 × 25 μm); **d**, C_{60} (optical micrograph, 8 × 8 μm).

rubrene-based transistor array yielded an average saturation regime mobility of $\sim 0.6 \pm 0.5\ cm^2\ V^{-1}\ s^{-1}$ with on/off ratios greater than 10^7 (Supplementary Fig. 10). These characteristics are comparable to those of amorphous silicon transistors and high-performance organic thin film transistors reported in the literature[25–27]. Pentacene single-crystal transistors were similarly fabricated using unpurified, as-received pentacene source material, with the resultant devices exhibiting mobilities on the order of $0.3\ cm^2\ V^{-1}\ s^{-1}$ and on/off ratios $>10^5$. The electrical characteristics of a typical pentacene device are displayed in Fig. 3c. Finally, devices made by patterning the n-channel materials C_{60} and TCNQ were found to exhibit mobilities of 0.03 and $10^{-4}\ cm^2\ V^{-1}\ s^{-1}$, respectively.

Our fabrication method can generate not only discrete single-crystal transistors on rigid SiO_2/Si substrates, but also flexible transistor arrays. The basic scheme for flexible single-crystal devices on a polyimide substrate and its realization with rubrene as the active material are shown in Fig. 4a (see also Methods for details). The characteristics of a selected plastic rubrene transistor before and after bending (stretching, bending direction across the channel) are presented in Fig. 4b. Mobilities as high as $0.9\ cm^2\ V^{-1}\ s^{-1}$ and on/off ratios of 10^4 (threshold voltage ~ 1.5 V) have been measured in our best flexible rubrene field-effect transistors, while our best mobility for a flexible pentacene field-effect transistor was $0.1\ cm^2\ V^{-1}\ s^{-1}$ with on/off ratios of $\sim 10^3$ (Supplementary Fig. 5). No significant loss in performance was observed when the devices were bent to a radius as small as 6 mm, as found in bending experiments performed on four randomly chosen devices that all exhibited similar behaviour. This demonstrates that the patterned single-crystal transistors can endure strenuous bending, and therefore are potentially useful for flexible electronics. Besides rubrene, high vapour pressure materials such as anthracene and tetracene were also successfully patterned on flexible and transparent poly(ethylene terephthalate) (PET) substrates without degrading the plastic (Fig. 4a).

The present results clearly show that the fabrication method we describe here can be used to control the nucleation location and nucleation density of molecular single crystals. But for the method to be technologically relevant, the orientation and alignment of the crystals also need to be controlled, because charge transport in single crystals can be highly anisotropic[7]. Preliminary results from our laboratory suggest that this is possible by using a combined nucleation/alignment layer. Another challenge is the need for a better understanding of the crystal growth mechanism in this system so as

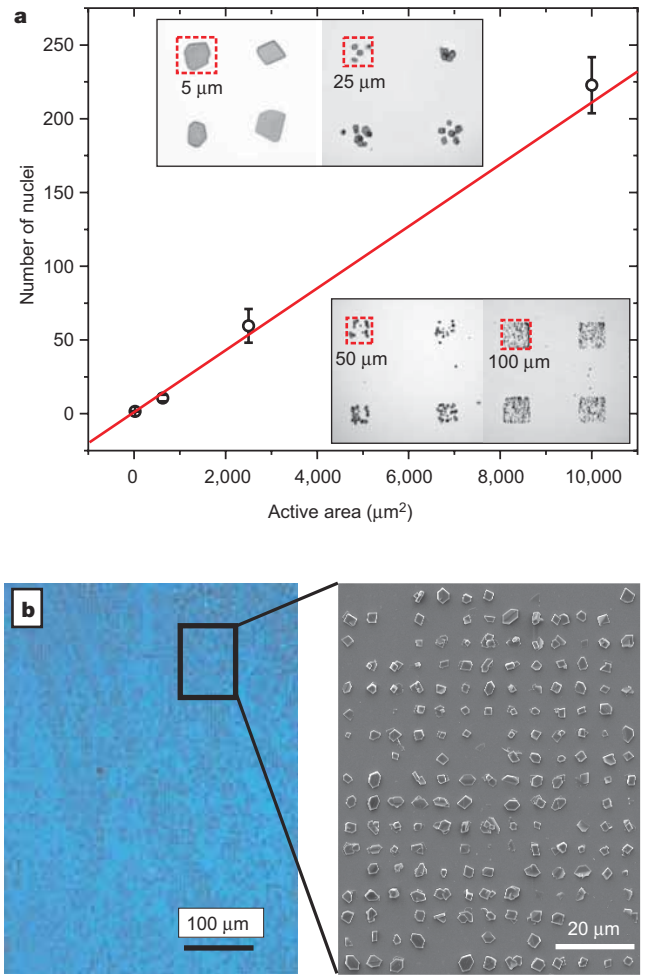

Figure 2 | Controlling pentacene crystal nucleation. The number of crystals nucleated and grown per stamped domain is a function of the domain area. **a**, Plot of the number of pentacene crystals in each stamped domain as a function of stamped domain area. The data points show the average crystal number found for the four different stamp sizes used in the experiment. The error bars indicate the standard error of the mean, obtained from counting the nuclei in 24 stamping domains of each size ($N = 24$). The red line is a linear fit of the experimental data, yielding a nucleation density value of one pentacene crystal per 49 μm² (equivalent to a stamping area of 7×7 μm). Insets, optical micrographs of the four different stamp sizes used. **b**, Example of a large-area array of discrete pentacene single crystals grown on a 5×5 μm stamped OTS pattern. The image on the left is an optical micrograph of the array, with the enlarged view of the indicated area shown as an SEM image on the right.

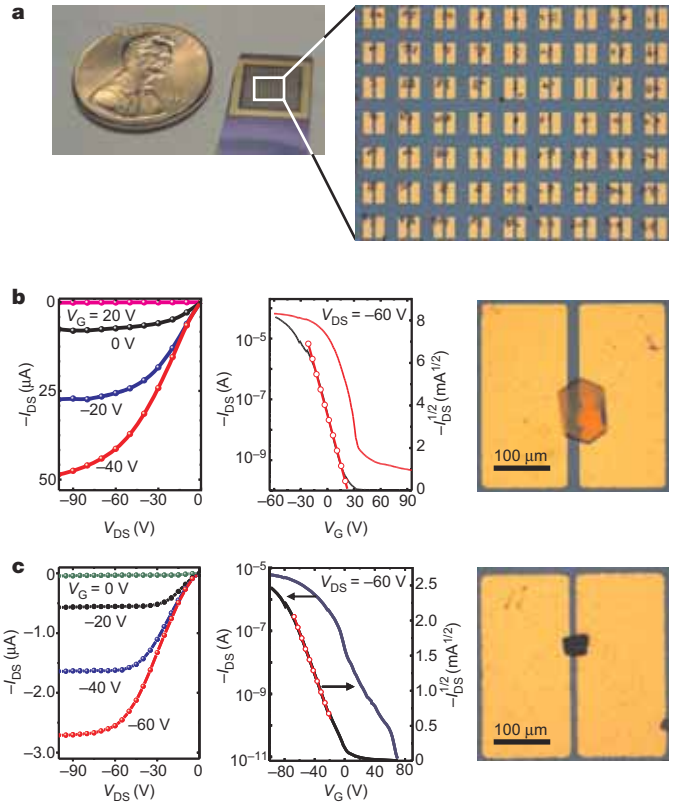

Figure 3 | Single-crystal transistor arrays on rigid substrates. Arrays of working single-crystal transistors are produced by printing films of OTS domains onto arrays of source–drain electrodes, followed by growth of organic single crystals in the printed domains. **a**, Optical micrograph of arrays of functional single-crystal transistors. The electrical characteristics of typical single-crystal transistors in the arrays, along with images of the transistors, are shown in **b** for rubrene, and in **c** for pentacene. V_{DS}, drain–source voltage; V_G, gate voltage; I_{DS}, drain–source current. Characteristics are as follows: **b** (middle panel), mobility (μ) = $2.4\ cm^2\ V^{-1}\ s^{-1}$, on/off ratio $\sim 10^6$, threshold voltage (V_{th}) = 22.4 V; **c** (middle panel), $\mu = 0.2\ cm^2\ V^{-1}\ s^{-1}$, on/off ratio $\sim 10^6$, $V_{th} = -3.1$ V.

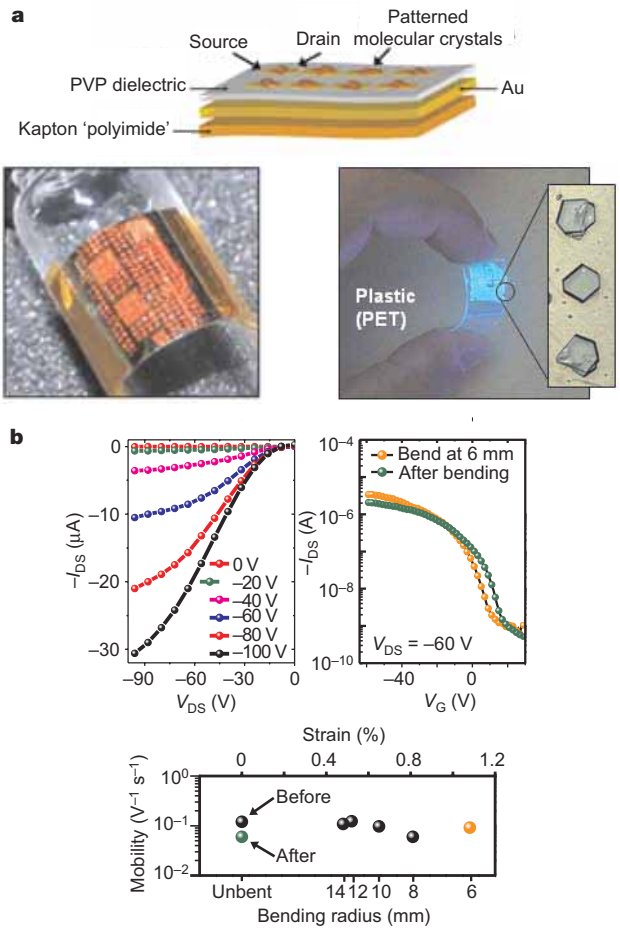

Figure 4 | Flexible single-crystal transistor arrays. a, Diagram of the basic design for single-crystal transistor arrays on plastic substrates (top). The optical micrographs (bottom) show a rubrene transistor array attached to a glass vial of diameter 11.7 mm (left), and anthracene crystals patterned on a poly(ethylene terephthalate) (PET) substrate and fluorescing under an ultraviolet light source (right). Patterned organic crystals were grown on flexible Kapton devices that were taped onto pre-cut glass microscope slides with high-temperature polyimide tape. **b**, Electrical characteristics of the single-crystal arrays. Left, the performance of a typical flexible rubrene single-crystal transistor. The middle and right panels illustrate the effect of device array bending on device performance. Middle, the transfer curves of a flexible device bent at 6 mm bending radius and after bending (that is, back in planar geometry); right, plot of mobility as a function of the bending radius (or strain percentage, which is indicated on the top axis). The green and orange curves in the middle panel correspond to the green and orange data points in the right panel. The electrical characteristics of all devices were first measured in the planar geometry, then repeatedly in the bent geometry, and finally again in the original planar geometry, similar to procedures used in ref. 28.

to optimize the electrical contact between the crystals and the dielectric layer, as well as between the crystals and the electrodes. Of course, practical applications in large-area flexible electronics will also require precise control of the growth process, to allow scaling of the fabrication method to larger areas while achieving high device uniformity and high device yield.

METHODS

Substrate patterning and crystal growth. OTS printing solutions were prepared in reagent grade toluene with concentrations ranging from 0.1 to 1.0 M. Cotton applicators were used to ink the PDMS stamps with the OTS solutions, and an air gun was used to dry the stamps from excess solvent. The stamps were brought into contact with substrates for approximately 5 min. No rinsing or heat treatment was administered to the OTS-patterned substrates. To deposit the crystals, we used a 16-mm-diameter glass tube that was open at one end and had already been closed (by flame-sealing) at the other. Semiconductor material was placed inside the tube near the closed end (~10 mg of source material used); the patterned substrate was put onto a NiCr wire clip and placed inside the tube, several centimetres away from the source material. Subsequently, the tube was completely flame-sealed under a vacuum pressure of ~0.38 mm Hg using a standard laboratory vacuum pump. As an example of the procedure used, the pentacene source temperature is maintained at ~260 °C and the closest edge of the patterned substrate is positioned 2 cm away (~250 °C) from the source zone. The nucleation zone of pentacene crystals extends to the far edge of the sample 5 cm away from the source (~220 °C). Next, the vacuum-sealed tube is placed into a temperature gradient sublimation reactor similar to the construction reported in ref. 16. Pentacene single crystals were grown in as little as 5 min with 5 μm stamps and in ~30 min using 100 μm stamps. Typical source temperatures for pentacene are ~260 °C. Growth temperatures for rubrene and C_{60} were 250–270 °C and 425–500 °C, respectively. Increasing the source temperature increases the rate of crystal growth, but also increases the distance from the source to the crystal-forming region. Calibration of materials under controlled parameters was conducted to determine the exact distance of crystal growth with respect to the source zone. Larger-diameter glass tubes were used in order to fabricate larger-area patterns. Organic source materials were purified by temperature gradient sublimation, but in most cases, they were used without any purification and used as received.

Device array fabrication. Bottom-contact devices (14 × 14 source–drain electrode arrays, channel lengths 10, 20, 50, 100 μm) were defined by conventional photolithography (metal thickness: Cr, 1.5 nm; Au, 40 nm). Single-crystal transistors were fabricated on conventional SiO_2 substrates containing a dielectric thickness of 300 nm on highly doped Si. A capacitance of 10 nF cm^{-2} was used to calculate the field-effect mobility of transistors on a 300 nm SiO_2 dielectric, whereas a capacitance of 1.9 nF cm^{-2} was used for 1.5-μm-thick poly-4-vinylphenol (PVP, M_w = 20,000) dielectric. For flexible transistors, a dielectric layer of PVP was spin-coated (~2,000 r.p.m.) on 140-μm-thick Kapton (polyimide) sheets covered with a 100 nm gold coating used for the gate electrode (Astral Technology Unlimited). The dielectric solution was prepared from 22 wt% PVP, and 8 wt% poly(melamine-*co*-formaldehyde), methylated (M_w = 511), dissolved in propylene glycol monomethyl ether acetate (PGMEA)[27]. The substrates were baked at 100 °C for 10 min then at 200 °C for 10 min to initiate crosslinking. The source–drain electrodes were fabricated by thermal evaporation of Cr (1.5 nm) and Au (50 nm) for flexible substrates. The W/L (W, channel width; L, channel length) for our highest mobility rubrene devices were ~2 for conventional SiO_2 substrates and ~4 for flexible polyimide devices. Patterned organic crystals were grown on flexible Kapton devices that were taped onto pre-cut glass microscope slides with high-temperature polyimide tape. All devices were first measured in the planar geometry mode followed by several bent geometry measurements, and finally measured in the original planar geometry, similar to procedures used in ref. 28.

Received 6 July; accepted 1 November 2006.

1. de Boer, R. W. I., Gershenson, M. E., Morpurgo, A. F. & Podzorov, V. Organic single-crystal field-effect transistors. *Phys. Status Solidi a* **201,** 1302–1331 (2004).
2. Briseno, A. L. *et al.* Patterned growth of large oriented organic semiconductor single crystals on self-assembled monolayer templates. *J. Am. Chem. Soc.* **127,** 12164–12165 (2005).
3. Huitema, H. E. A. *et al.* Plastic transistors in active-matrix displays. *Nature* **414,** 599 (2001).
4. Moon, H. *et al.* Synthesis, crystal structure, and transistor performance of tetracene derivatives. *J. Am. Chem. Soc.* **126,** 15322–15323 (2004).
5. Podzorov, V. *et al.* Intrinsic charge transport on the surface of organic semiconductors. *Phys. Rev. Lett.* **93,** 086602 (2004).
6. Pope, M., Charles, E. & Swenberg, C. E. *Electronic Processes in Organic Crystals and Polymers* (Oxford Univ. Press, New York, 1999).
7. Sundar, V. C. *et al.* Elastomeric transistor stamps: Reversible probing of charge transport in organic crystals. *Science* **303,** 1644–1646 (2004).
8. Zeis, R. *et al.* Field effect studies on rubrene and impurities of rubrene. *Chem. Mater.* **18,** 244–248 (2006).
9. Steudel, S., Janssen, D., Verlaak, S., Genoe, J. & Heremans, P. Patterned growth of pentacene. *Appl. Phys. Lett.* **85,** 5550–5552 (2004).
10. De Vusser, S., Steudel, S., Myny, K., Genoe, J. & Heremans, P. Integrated shadow mask method for patterning small molecule organic semiconductors. *Appl. Phys. Lett.* **88,** 103501 (2006).
11. Aizenberg, J., Black, A. J. & Whitesides, G. M. Controlling local disorder in self-assembled monolayers by patterning the topography of their metallic supports. *Nature* **394,** 868–871 (1998).
12. Aizenberg, J., Black, A. J. & Whitesides, G. M. Control of crystal nucleation by patterned self-assembled monolayers. *Nature* **398,** 495–498 (1999).
13. He, J. H. *et al.* Pattern and feature designed growth of ZnO nanowire arrays for vertical devices. *J. Phys. Chem. B* **110,** 50–53 (2006).

14. van der Wilt, P. C., van Dijk, B. D., Bertens, G. J., Ishihara, R. & Beenakker, C. I. M. Formation of location-controlled crystalline islands using substrate-embedded seeds in excimer-laser crystallization of silicon films. *Appl. Phys. Lett.* **79,** 1819–1821 (2001).
15. Vikas, R. *et al.* in *Proc. International Electron Devices Meeting 2005* 919–922 (IEEE International, 2005).
16. Kloc, C., Simpkins, P. G., Siegrist, T. & Laudise, R. A. Physical vapor growth of centimeter-sized crystals of alpha-hexathiophene. *J. Cryst. Growth* **182,** 416–427 (1997).
17. Choi, H. Y., Kim, S. H. & Jang, J. Self-organized organic thin-film transistors on plastic. *Adv. Mater.* **16,** 732–736 (2004).
18. Ruiz, R. *et al.* Pentacene thin film growth. *Chem. Mater.* **16,** 4497–4508 (2004).
19. Heringdorf, F., Reuter, M. C. & Tromp, R. M. Growth dynamics of pentacene thin films. *Nature* **412,** 517–520 (2001).
20. Markov, I. V. *Crystal Growth for Beginners* (World Scientific, Singapore, 2003).
21. Venables, J. A., Spiller, G. D. T. & Hanbucken, M. Nucleation and growth of thin films. *Rep. Prog. Phys.* **47,** 399–459 (1984).
22. Granasy, L., Borzsonyi, T. & Pusztai, T. Nucleation and bulk crystallization in binary phase field theory. *Phys. Rev. Lett.* **88,** 206105 (2002).
23. Granasy, L. *et al.* Phase field theory of crystal nucleation and polycrystalline growth: A review. *J. Mater. Res.* **21,** 309–319 (2006).
24. Verlaak, S., Steudel, S., Heremans, P., Janssen, D. & Deleuze, M. S. Nucleation of organic semiconductors on inert substrates. *Phys. Rev. B* **68,** 195409 (2003).
25. Kelley, T. W. *et al.* Recent progress in organic electronics: Materials, devices, and processes. *Chem. Mater.* **16,** 4413–4422 (2004).
26. Klauk, H., Gundlach, D. J., Nichols, J. A. & Jackson, T. N. Pentacene organic thin-film transistors for circuit and display applications. *IEEE Trans. Electron Devices* **46,** 1258–1263 (1999).
27. Klauk, H. *et al.* High-mobility polymer gate dielectric pentacene thin film transistors. *J. Appl. Phys.* **92,** 5259–5263 (2002).
28. Briseno, A. L. *et al.* High-performance organic single-crystal transistors on flexible substrates. *Adv. Mater.* **18,** 2320–2324 (2006).

Supplementary Information is linked to the online version of the paper at www.nature.com/nature.

Acknowledgements A.L.B. acknowledges a Bell Labs Graduate Research Fellowship. A.L.B., F.W., R.J.T. and Y.Y. acknowledge financial support from the Air Force Office of Scientific Research (AFOSR). S.C.B.M. acknowledges financial support from the Deutsche Forschungsgemeinschaft, and Z.B. acknowledges partial support from the Stanford Center for Polymeric Interfaces and Macromolecular Assemblies (NSF-Center MRSEC), the Stanford School of Engineering, and a Sloan Research Fellowship.

Author Contributions A.L.B. performed single-crystal patterning on substrates and FET devices, measurements on FET devices, and wrote most of the manuscript. S.C.B.M. elucidated the growth mechanism, performed AFM measurements, and wrote parts of the manuscript. M.M.L. assisted in sample preparation and assisted in device measurements and calculations. S.L. assisted in crystal patterning, device preparation, and performed SEM measurements. R.J.T. assisted in flexible device preparation, measurements and calculations. C.R. designed and fabricated the transistor array devices and PDMS stamp masters via lithography. M.E.R. assisted in early experiments and purified some of the organic source materials. Y.Y. provided use of laboratory space and instruments. F.W. provided feedback and suggestions on experiments. Z.B. conceptualized and directed the research project. All authors discussed the results and commented on the manuscript.

Author Information Reprints and permissions information is available at www.nature.com/reprints. The authors declare no competing financial interests. Correspondence and requests for materials should be addressed to Z.B. (zbao@chemeng.stanford.edu).